

Ascending-descending orbit combination SAR interferometry assessment

Daniel Carrasco, Javier Díaz & Antoni Broquetas

*D3-EEF Electromagnetic Engineering & Photonics Group, Signal Theory & Communications Dept.
Universitat Politècnica de Catalunya. Gran Capitán, Campus Nord D3, 08034 Barcelona, Spain*

Tel. +34 3 4016849 Fax: +34 3 4017232

<http://www.gaig.upc.es> www.tsc.upc.es/d3eef - diaz@volor.upc.es

Roman Arbiol, Manuel Castillo & Vicenç Palà

Institut Cartogràfic de Catalunya. Parc de Montjuïc s.n. 08004 Barcelona. Spain

Tel. +34 3 4252900 Fax: +34 3 4267442 - <http://www.icc.es>

Abstract

Ascending-descending orbit combination for DEM generation is very promising technique which can be used to fill in some gaps in the DEMs caused by the geometric deformations or SAR images. The benefits from the combination over layover and foreshortening areas are evident thanks to the new data made available over these areas from the opposite pair. However, other areas in the image will also improve its quality because of the averaging between the ascending and the descending pass. This paper shows an ascending descending orbit combination using ERS data. Two ascending and descending DEMs have been calculated independently and a combined DEM has been obtained from them on a coherence basis. The obtained DEMs have been compared with a high accuracy DEM (2m height rms) available. Results show an error reduction in the combined DEM over the ascending and descending ones.

Keywords: SAR Interferometry, DEM, ascending-descending orbit combination.

Introduction

Obtaining digital elevation models (DEM) with interferometric techniques has become one of the major potential applications of SAR satellites. SAR interferometry process basis has been widely described and assessed (Zebker 94, Massont 93, Prati 94, Carrasco 95). Due to the SAR looking geometry some deformations appear in SAR images in mountainous areas. When the slope facing the radar, approaches the value of the sensor off-nadir angle (23° for the ERS-1) it is too hard to obtain height information, for all the slope is concentrated in a few pixels of the image (foreshortening) and there may not be interferometric information at all. When this slope exceeds the off-nadir angle layover effect arises in SAR images. However, these hilly areas can be recovered by looking from to the opposite site, i.e. by using another interferometric pair acquired from the opposite direction. Therefore, the foreshortening and layover problems, related to SAR looking geometry, can be solved by combination of ascending and descending orbits over the same ground scene, since the layover or foreshortening problematic areas in one of the interferograms would be easy to recover in the other one as it has been done in (Pascuali, 94). However, as it will be shown, there is also a quality improvement outside of these critical areas.

An experiment with SAR data acquired by the ERS-1 close to Tarragona in Catalonia (Spain) has been carried out. The test site is by the side of the river Ebro. Two elevation maps are generated: one from an ascending orbit pair and other from a descending one. A combined DEM is obtained from both elevation maps. Finally the three elevation maps are compared with a high accuracy reference DEM, for the sake of assess the achieved results.

Experiment over Catalonia

Amplitude detected images of the ascending and descending passes are shown in figures 1 and 2. The ascending pair corresponds to 3-day repeat pass orbit and the descending one to 35-day repeat pass orbit. It is easy to notice the course of the river (darker than the rest of the image) which will be exploited as a reference. Baselines have been estimated and they are approximately 157 and 152 meters for ascending and descending pairs respectively.

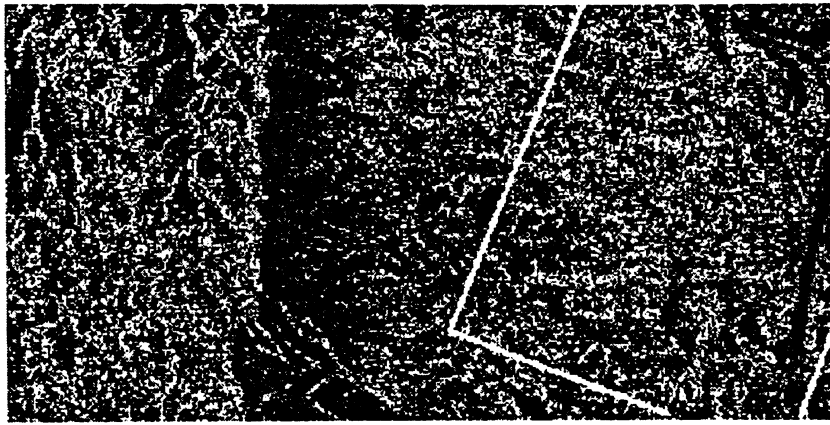


Fig. 1. ERS-1 ascending pass image (azimuth: 4.5 Km; range: 9 Km). The area which overlaps the descending image has been remarked.

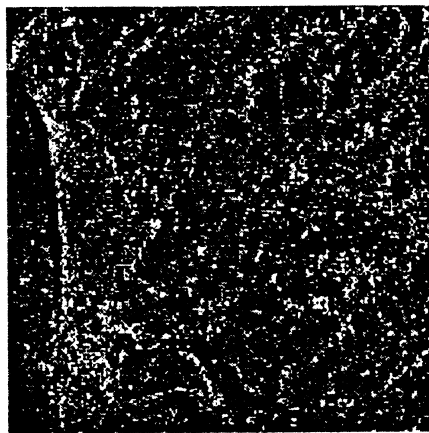


Fig. 2. ERS-1 descending pass image (4.5 x 4.5 Km)

The interferometric processing is applied independently over the two pairs of images (ascending and descending). The two resulting interferograms, after flat Earth removal and adaptive fringe filtering, are shown in figures 3 and 4. Despite of the filtering, it can be seen that the 35 day pass descending interferogram is much noisier than the 3 day pass descending one because of the coherence loss. Phase unwrapping is performed using a least squares algorithm (Ghiglia, 94) (Pritt, 94) and after the phase to height conversion and projection over ground range, two DEM are obtained (see figures 5 and 6).

Now, with the best information from each of these two DEMs, a combined elevation model must be generated. In order to associate each point in one image with its equivalent in the other one, a ground control point grid is needed to determine the translation, rotation and stretching parameters needed to superimpose both DEMs one over the other (notice this can only be done after slant to ground-range conversion). These ground control points are local maxima in the DEMs. Once that both DEMs are over the same grid, it is necessary a criterion to choose either a point in the first DEM or its equivalent in the second DEM (or a weighted combination of both points) to generate the final DEM (see figure 7). Following the approach proposed in (Pascuali, 94), the height from the best coherence is selected. Should coherence be over a predefined threshold in both interferograms, a weighted value will be selected, else the best coherence point will be used. Before the combination, the coherence maps should be averaged to prevent from data chopping.

The three resulting DEMs (ascending, descending and combined) have been compared to a high accuracy reference DEM which has a 2m rms. height error and 15m by 15m grid provided by the Institut Cartogràfic de Catalunya.

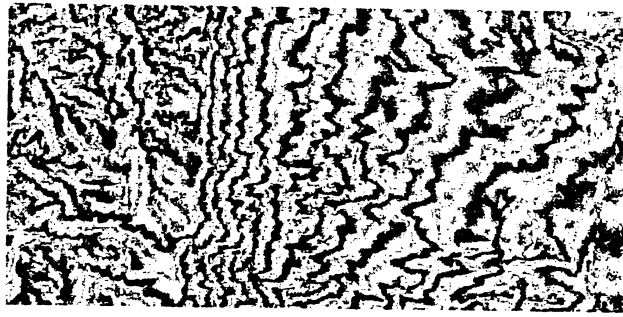


Fig. 3. Ascending pass interferogram.

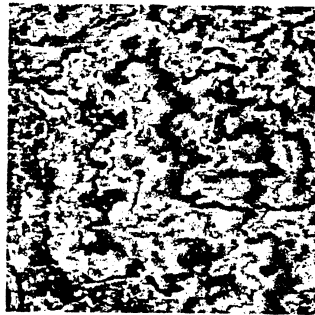


Fig. 4. Descending pass interferogram.

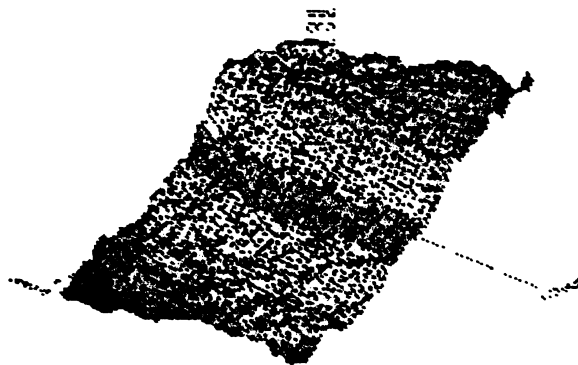


Fig. 5. Ascending 3D elevation map

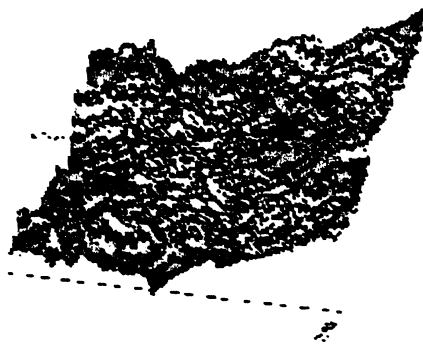


Fig. 6. Descending 3D elevation map

The three DEMs have been translated, rotated and stretched so that they sized the reference DEM. Then, the absolute heights in the SAR DEMs were obtained by adding a constant in order to achieve the same average height in all of them. The absolute value of the difference between the DEMs was computed and the result is shown in Fig. 8. Differences elevation maps vary from blue (less than 5 m) to red (over 40 m). Table I summarises the values of the medium and rms. errors. It is worthy of notice the improvement achieved through the DEM combination, more clearly noticeable in the accumulative frequency error diagram shown in Fig. 9.



Fig 7. Combination of ascending and descending passes.

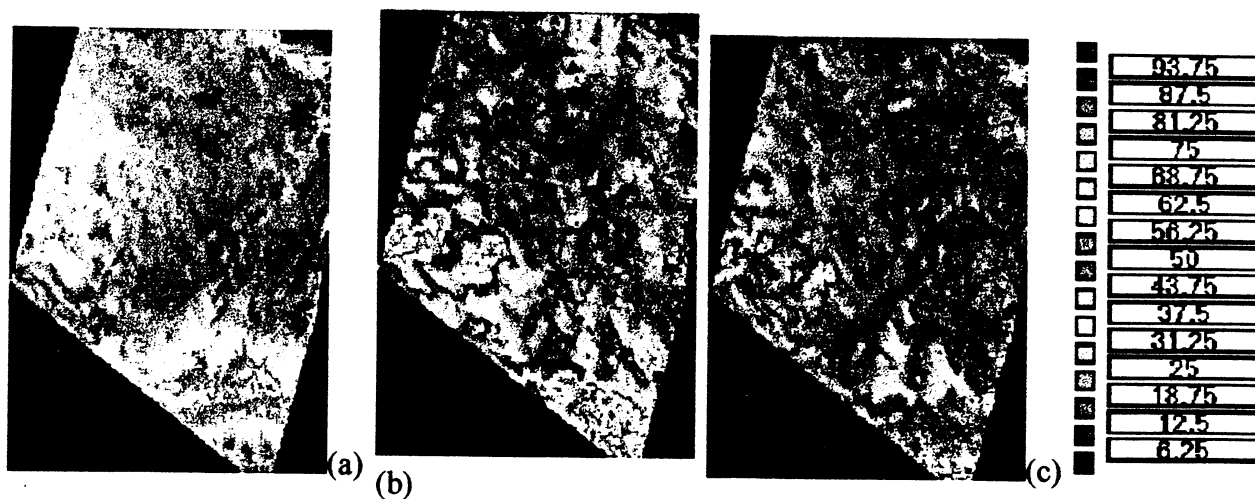


Fig 8 Absolute error between the InSAR DEMs and the reference DEM. (a) is related to the ascending DEM, (b) to descending and (c) correspond to the combination.

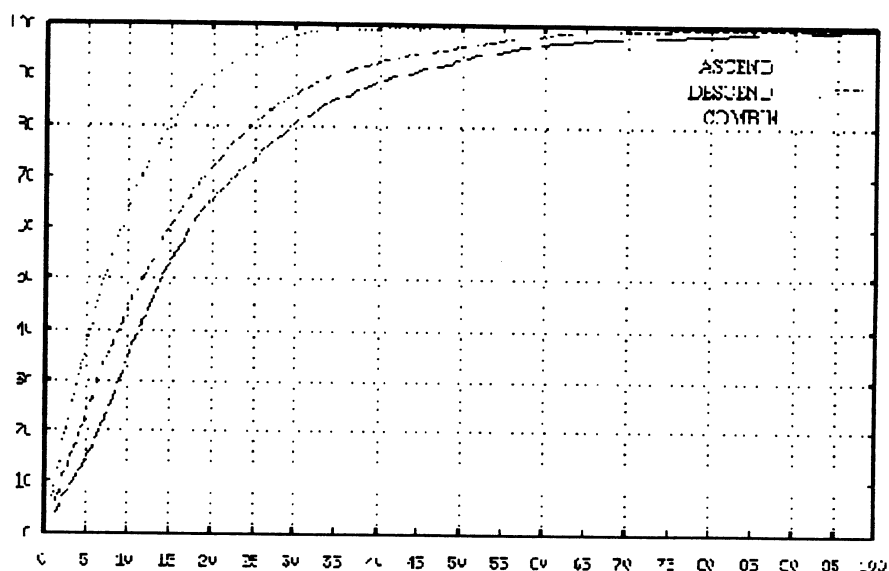


Fig. 9 Comparison between accumulative frequency error diagrams (% of points vs error in meters).

	Ascending	Descending	Combined
Mean abs. error	19.2 m	16.1 m	9.1 m
RMS error	24.4 m	21.3 m	12.0 m

Table I Values of the mean absolute error and the RMS error from the ascending, descending and combined error maps.

Conclusions

It has been demonstrated that the ascending-descending orbit combination method can be useful for DEM generation even outside of high foreshortening or layover areas. The coherence based height average chooses the best of each DEM lowering the total error.

The rotation of one DEM over the other one is a critical step. Since one DEM must be superimposed over the other in ground range, the unwrapped phase should not have propagated errors in order to allow the matching of both DEM. This could be accomplished at hilly sites by masking the difficult areas. The rotation using local maxima ground control points requires operator intervention for their location. Further work is being addressed to automate the ascending-descending matching on a correlation basis.

Acknowledgement

The authors would like to thank the European Space Agency ERS-Fringe working group for providing the ERS data used in this work which has been carried out in the frame of the TANDEM project AO2/E105. This work has been supported by the Comisión Interministerial de Ciencia y Tecnología CICYT - TIC 96-0879.

References

1. Zebker, C. Werner, P. Rosen, S. Hensley: *Accuracy of Topographic Maps Derived from ERS-1 Interferometric Radar*. IEEE Trans. GRS, Vol. 32, N° 4, July 1994, pp. 823-836.
2. Massonet, T. Rabaute: *Radar Interferometry: Limits and Potential*. IEEE Trans. GRS, vol. 31, N° 2, pp. 455-464, Mar. 1993.
3. Prati, F. Rocca, A. Monti Guarnieri, P. Pascuali: *Report on ERS-1 SAR Interferometric Techniques and Applications*. ESA Contract n. 3-7439/92/HGE_I. June, 94.
4. Carrasco, J. Alonso, A. Broquetas:

Accuracy of SAR interferometry using the ERS-1, IEEE International Geoscience and Remote Sensing Symposium 1995 Proceedings. Florence 1995, pp. 781-783D. Ghiglia, L. Romero: *Robust two-dimensional weighted and unweighted phase unwrapping that uses fast transforms and iterative methods*. J. Opt. Soc. Am A, Vol. 11, N° 1, Jan. 1994, pp. 107-117.

1. Pritt, J. Shipman: *Least-Squares Two-Dimensional Phase Unwrapping Using FFT's*. IEEE Trans. on GRS, Vol. 32, N° 3, May 1994, pp. 706-708.

P. Pascuali, R. Pellegrini, C. Prati, F. Rocca:

Combination of interferograms from ascending and descending orbits. IGARSS 94, Vol. 2, pp. 733-735.